7-1988

State of the Art in Swath Bathymetry Survey Systems

Christian de Moustier
University of California - San Diego

International Hydrographic Review, Monaco, LXV(2), July 1988

STATE OF THE ART IN SWATH BATHYMETRY SURVEY SYSTEMS

by Christian de MOUSTIER (*)

Paper originally presented at the symposium on 'Current Practices and New Technology in Ocean Engineering' held by the American Society of Mechanical Engineers (ASME) in New Orleans, Louisiana, 10-13 January 1988, and reprinted with the kind authorization of the symposium's organizers.

Abstract

In the last decade, advances in real-time computing and data storage capabilities have led to significant improvements in bathymetric survey systems and the single point echo-sounder has now been replaced by a variety of high-resolution swath mapping sounding systems. This paper reviews the state of the art in the non-military swath bathymetry mapping systems. Such systems are typically multi narrow beam echo-sounders or interferometric side-looking sonars with swath width capabilities ranging from 0.75 to 7 times the water depth. The paper compares the design characteristics and the echo processing methods used in a number of these systems manufactured in Japan, Finland, Norway, the U.K., the U.S.A. and West Germany.

1. INTRODUCTION

The outcome of a bathymetric survey is a map of water depths in a geographic reference frame. In rivers, estuaries, navigational channels, harbors and in shallow coastal waters, concerns for navigational safety underscore the need for such surveys. In the open ocean, the incentive for bathymetric surveys is mostly of an exploratory nature, although seamounts are potentially hazardous to submarine navigation. Knowledge of seafloor relief helps marine geologists draw inferences on the dynamic processes that shape the Earth. It also helps establish the feasibility of offshore exploration of mineral deposits, particularly in the Exclusive Economic Zones claimed by countries with oceanic borders.

(*) Marine Physical Laboratory, Scripps Institution of Oceanography, University of California, San Diego, La Jolla, California 92093, USA.

Until the 1920's, water depth was measured by the lead and line method and although the measurements were reliable, their spacing usually under-sampled the bottom relief giving the false impression of featureless seabeds. In the 1920's echo-sounders began to replace the lead line and nearly continuous records of depth along each traverse of the ship became possible. In the 1950's, improvements in transducer technology and in timing accuracy brought about the precision depth sounder and recorder, commonly known as PDR's [1]. These echo-sounders highlighted the varied relief found on the bottom of the oceans, but because of their broad beamwidth (30-60°) they could only delineate the large scale relief (> 1 km). To remedy this shortcoming, narrow beam echo-sounders (2-3°) with mechanical stabilization against roll were introduced in the late 1950's.

To produce a 2° beamwidth at the sounding frequencies commonly used (10-15 kHz), the acoustic arrays need to be over 3 m in length (compared to 25 cm for wide beam transducers) making the mechanical stabilization difficult. Electronic stabilization schemes using array phasing networks were proposed in 1960 [2] and alternatives to the large acoustic arrays were investigated with directional echo-sounders based on the interferometric technique, which uses the phase difference produced by an echo received at 2 vertically separated arrays to determine its angle of arrival [3].

With the narrow beam echo-sounder, relief from meters to kilometers can be recorded as a continuous profile along the ship's track. However, for bathymetric survey work, several parallel profiles are needed to create a map and the accuracy of the ship's navigation becomes a critical factor. In addition, for economic reasons, profiles are usually spaced kilometers apart resulting in under-sampling of the relief in the transverse direction. To overcome this problem, a number of parallel sounding methods have been devised. These methods include mounting several transducers on long booms extending abeam of the survey vessel [4], mounting transducers in tow bodies to be towed in parallel from a single ship [5], or outfitting small launches with echo-sounders and navigating the launches in parallel formation with a mother ship [6]. However, these methods are only applicable to calm weather environments as they are limited by the sea-worthiness of both operators and equipment as well as by the difficulties associated with deployment and navigation. Note that a project currently under development in Canada plans to expand on the parallel sounding method by replacing the manned launches by diesel powered remotely operated vehicles [7].

The next advance in bathymetric survey methods came from the concepts of multiple-beam echo-sounders [8, 9] and of multi narrow beam echo-sounders that measure depths simultaneously from a series of beams pointing at discrete angles of incidence in the athwartship direction. The latter was brought to production with the Sonar Array Sounding System (SASS) [10, 11], a classified multibeam bathymetric swath survey system, by the General Instrument Corporation (GIC) which patented it in 1964. However, it was not until the mid-70's, with the advances in real-time computing and data storage capabilities, that commercial versions of this system became available. GIC manufactured two such systems, Sea Beam for deep water applications and Hydrochart for shallow water [12, 13]. The Sea Beam system has since been installed on a dozen ships worldwide and it has revolutionized the way in which bathymetric surveys are run. In its wake, a number of multibeam echo-sounding systems have been

developed and manufactured during the last five years in West Germany (Hydrosweep, Bottom Chart), Finland (Echos XD), Norway (EM 100, Benigraph) and Japan (MBSS).

In parallel with the development of multibeam echo-sounders, applications of the phase measuring interferometer concept started with an experimental sidescan interferometer system for obstacle avoidance [14]. By the mid 1970's, the Telesounder [15] used the fringes produced by an acoustic version of the Lloyd Mirror effect to measure bathymetry across track. This concept was also implemented more recently in an interferometric sidescan sonar system (ISSS) [16], however, the signal processing required for automatic detection of the interference fringes and the corresponding depth computations are too extensive to be done in real time and a relatively limited number of depth samples are obtained for each transmission cycle. By contrast, phase measuring bathymetric sidescan systems have the potential to provide hundreds of depth points across track. An experimental version of such a system designed for shallow water applications and operating at 410 kHz was presented in 1977 by DENBIGH [17]. Similar shallow water bathymetric sidescan systems were developed in the U.K. (Bathyscan) [18, 19, 20] and Norway (Topo-SSS) [21] between 1979 and 1985. In the early 1980's a collaborative effort between the International Submarine Technology Corporation (IST) and the Hawaii Institute of Geophysics (HIG) developed the interferometric technique into a member of the Sea Mapping and Remote Characterization (SeaMARC) family of sonar systems built by IST. This system, known as SeaMARC II, combines high resolution sidescan imagery of the seafloor with swath bathymetry capabilities [22]. Today it is the only deep ocean system of this kind in operation. The team who developed the SeaMARC II has recently introduced the SeaMARC/S, a high resolution version designed for mid to shallow water surveys [23]. This new system is owned and operated by Seafloor Surveys International (SSI) in Honolulu, Hawaii.

In the following, we compare the bathymetric swath mapping capabilities of eight non-military, multi narrow beam echo-sounders and three towed interferometric sidescan sonars. Because some of these systems are relatively new and have insufficient field records, the discussion is confined to the hardware and processing methods rather than the resulting bathymetric data. To help to understand the different design philosophies implemented in these systems, we first give a brief theoretical background on the constraints to be dealt with in designing a swath bathymetric survey system.

2. THEORY OF OPERATION

In this section we briefly review the theory of operation applicable to multi narrow beam echo-sounders and to interferometric sidescan sonars. Note that the following discussion applies to single frequency systems and narrow band signals so that phase delays and time delays can be used interchangeably.

Multi narrow beam systems are based on the cross fan beams geometry created by two transducer arrays mounted at right angles to each other in an L or

a T configuration. Each array produces a beam which is narrow in the direction perpendicular to its short axis. The intersection of the two resulting patterns is a beam delimited by the narrow widths of these patterns. In practice the arrays are made up of a number of identical transducer elements equally spaced and driven individually or in subgroups to allow for sidelobe control and for steering of the mainlobe. The beam pattern $P(\theta, \phi)$ in the far field of such an array is computed by multiplying the pattern $f(\theta, \phi)$ of a single transducer element or subgroup by the pattern $g(\theta, \phi)$ of an array of point sources located at the center of each transducer element or subgroup:

$$P(\theta,\phi) = f(\theta,\phi) \times g(\theta,\phi) \tag{1}$$

where θ is the depression angle from the normal to the face of the array, and ϕ is the azimuthal angle. In the following, we are mostly concerned with the dependence of the radiation pattern in θ. In the ϕ dimension, the pattern depends on the width of the element or subgroup and the corresponding shaping effects can be included as a separate multiplicative term.

The pattern of a single element of length l has the form

$$f(\theta) = \frac{\sin x}{x}, \qquad x = \pi \frac{l}{\lambda} \sin\theta \tag{2}$$

where λ is the acoustic wavelength. For a line array with N omnidirectional elements equally spaced a distance d apart

$$g(\theta) = \sum_{n=0}^{N-1} A_n e^{jn\Psi} \quad \text{with} \quad \Psi = 2\pi \frac{d}{\lambda} \sin\theta \tag{3}$$

where A_n is the amplitude coefficient of the n^{th} element and θ is the angle from the normal to the face of the array in the plane containing its long axis. Note that complex notation is used here for ease of writing, the magnitude of the complex function gives the actual radiation pattern (see Appendix).

This pattern is periodic in Ψ with period 2π, it has a mainlobe corresponding to its maximum at $\Psi = 0$, it has $(N - 2)$ sidelobes (secondary lobes) within each period, and its norm is symmetric about $\Psi = \pi$. It is therefore fully defined for values of Ψ in the interval $[0,\pi]$. The corresponding values of θ are such that

$$0 \leqslant 2\pi \frac{d}{\lambda} \sin\theta \leqslant \pi \tag{4}$$

As the region of interest for this radiation pattern is the half space in front of the array, θ varies from $-\pi/2$ to $+\pi/2$. According to Eq. (4), $g(\theta)$ is then fully defined in the interval $[0,\pi/2]$ when $d \leqslant \lambda/2$. This is the spatial sampling equivalent of the Nyquist sampling criterion for time series. When the element spacing is greater than $\lambda/2$, the pattern $g(\theta)$ repeats itself in the interval $[0,\pi/2]$ and grating lobes (repetition of the mainlobe) appear at values of θ which render the argument Ψ an integral multiple of 2π:

$$\theta = arcsin\,(m\frac{\lambda}{d}),\ (\mid m\frac{\lambda}{d}\mid \leqslant 1)\ m\ integer \tag{5}$$

Beam steering is used to ensure that the mainlobe of the transmit beam pattern is oriented vertically down or to generate multiple receive beams. To steer a beam in the angular direction θ_i, the phase of the signal on each array element or subgroup is modified by the factor:

$$\Psi_i = 2\pi\frac{d}{\lambda}\sin\theta_i \tag{6}$$

so that signals arriving or departing in the direction θ_i appear in phase at all the elements of the array. Eq. (3) is therefore rewritten:

$$g(\theta) = \sum_{n=0}^{N-1} A_n\, e^{jn(\Psi - \Psi_i)} \tag{7}$$

At the half power point (−3dB), the width of the mainlobe of a beam steered in the direction θ_i is roughly equal to the reciprocal of the number of wavelengths across the effective aperture of the array. The beamwidth expressed in radians is then:

$$\theta_{-3dB} = \frac{\lambda}{(N-1)d\cos\theta_i} \tag{8}$$

As a result, the mainlobe widens as the steering angle increases from broadside ($\theta_i = 0^o$) to endfire ($\theta_i = 90^o$). Eq. (8) also entails that the beamwidth decreases as the number of elements N is increased or, if N is fixed, for increasing element spacing d. However, for echo-sounding applications it is important to minimize the effects of the grating lobes by choosing d (Eq. 5) such that the grating lobes fall outside of the angular region of interest.

To avoid grating lobes in steered beams, the argument $(\Psi - \Psi_i)$ must be less than or equal to the last null of the function $g(\Psi)$ (right side of Eq. 7):

$$-2\pi\frac{(N-1)}{N} \leqslant (\Psi - \Psi_i) \leqslant 2\pi\frac{(N-1)}{N} \tag{9}$$

Note that for a broadside beam ($\Psi_i = 0$) this condition violates the Nyquist criterion for spatial sampling. However, because no grating lobes appear in the visible region and because sidelobes can be controlled by amplitude shading, under-sampling with an element spacing slightly less than λ (i.e. $(N-1)\,\lambda/N$) is acceptable. This is analogous to an under-sampled time series which is narrowband and centered at DC; as long as the aliased portion remains outside of the band of interest, under-sampling is viable. From the definitions of Ψ and Ψ_i (Eq. 3 & 6), Eq (9) implies that, in order to steer a beam in the interval $[-\pi/2, +\pi/2]$ corresponding to the visible region or the half space in front of the array,

the element spacing d must satisfy;

$$d \leqslant \frac{(N-1)}{N} \frac{\lambda}{2} \tag{10}$$

Another common method of beam steering uses the properties of the discrete Fourier transform (DFT) by replacing the phase term Ψ_i in Eq. (7) and (9) by

$$\Psi_m = -\frac{2\pi m}{N}, \qquad m = -N/2, \ldots, 0, \ldots, (N/2-1) \tag{11}$$

The resulting beams are steered in the directions θ_m such that

$$\theta_m = arcsin\left(\frac{\lambda m}{Nd}\right), \left|\frac{\lambda m}{Nd}\right| \leqslant 1 \tag{12}$$

Note that with this method of beam steering, beams are not all equally spaced in angle over the visible region. For example, a 64 element array with $\lambda/2$ element spacing has equally spaced beams within $\pm 20°$ of broadside only.

Sidelobes are also a concern in echo-sounding and, for an array of equal amplitude elements, the first sidelobes appear about 13 dB below the mainlobe. To achieve greater sidelobe control, it is customary to apply an amplitude shading function to the array coefficients A_n (Eq. 3). This is equivalent to multiplying the pattern $g(\theta)$ of an array of equal amplitude elements by a window $w(n)$. A variety of windows [24] are effective in reducing the sidelobe level of the radiation pattern. However, sidelobe reduction is often accompanied by a broadening of the mainlobe. For narrow beam echo-sounders, the Dolph-Chebyschev window provides an optimum sidelobe reduction level for a given width of the mainlobe [25].

Further incentive to lower the sidelobe levels of the arrays is warranted by the fact that when multiple beams are formed by electronic steering, the mainlobe of any one beam points in the same direction as one of the sidelobes from each of the other beams. As a result, poor sidelobe control can seriously degrade the angular resolution of a multibeam echo-sounder and affect the depth determination accordingly. As an example, the theoretical cross fan beams geometry used in the Sea Beam systems is illustrated in Figure 1.

By contrast, interferometric sidescan sonars use a single fan beam generated by a transducer array whose long axis is parallel to the direction of travel. The resulting radiation pattern follows Eq. (1-3). It is wide in the vertical direction and narrow in the horizontal direction. The interferometric effect is used for reception only and it is obtained by mounting two such arrays parallel to each other with their centers a vertical distance D apart. Angular resolution is then achieved by relating the phase difference of signals arriving at the two arrays to the angle of arrival of these signals. This is in essence a reverse beamforming operation based on the assumption that the wavefront reaching the arrays originated from a small area on the seafloor so that the signals received at the

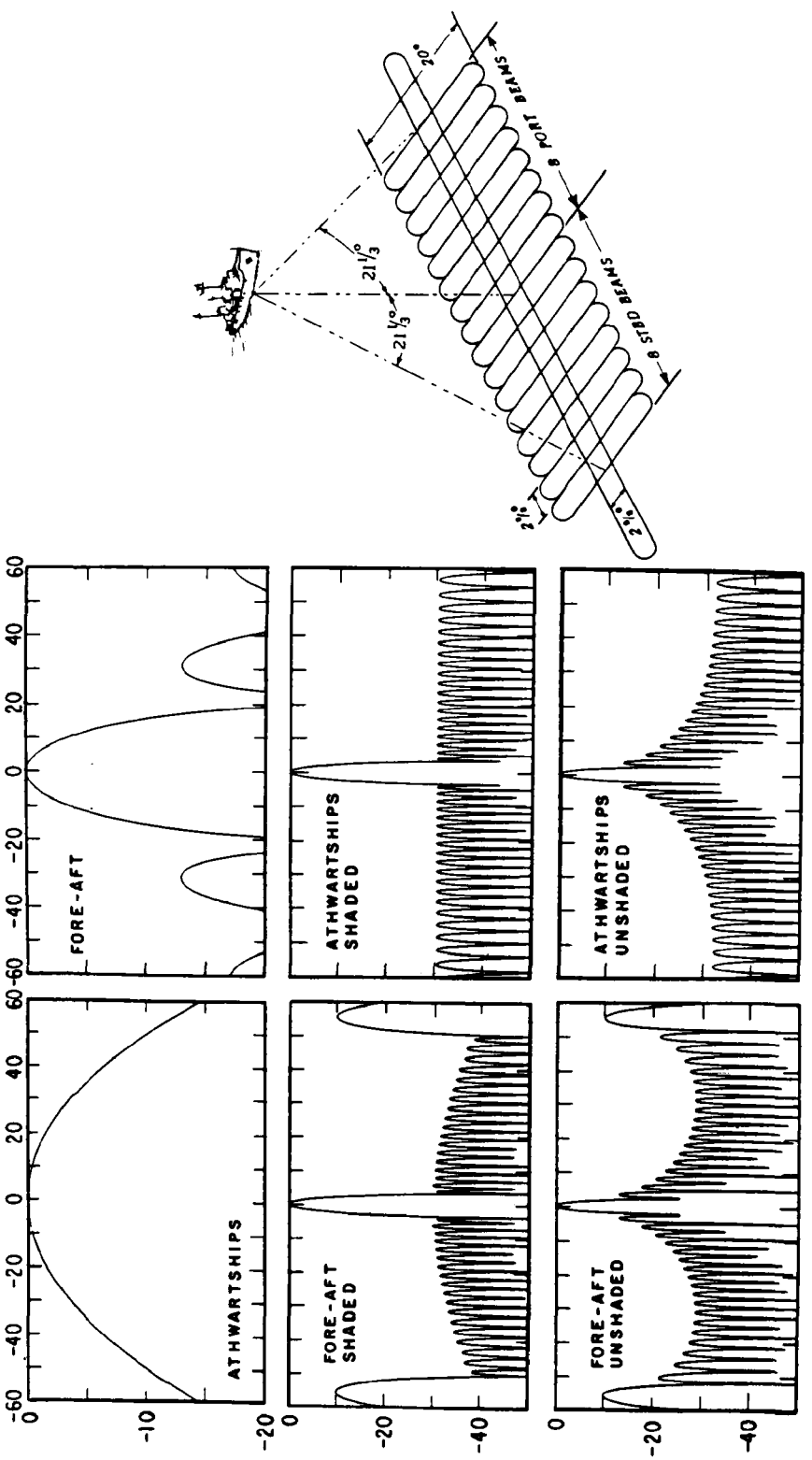

FIG. 1. — Theoretical radiation pattern for the Sea Beam system: (a) Transmit, (b) Receive, (c) Cross fan beam geometry (from de MOUSTIER and KLEINROCK [27]).

two arrays have a high degree of spatial coherence. The arrival angle θ of the wavefront with respect to the normal to the plane containing the two arrays is then obtained from Eq. (6) by substituting the vertical spacing D of the arrays for the element spacing d and the phase difference ϕ for the phase factor Ψ_i:

$$\phi = 2\pi \frac{D}{\lambda} \sin\theta \tag{13}$$

Eq. (13) implies that the angular resolution of the system increases with the separation of the arrays. However, phase can only be measured to 2π, thus the angular sector over which unambiguous phase measurements are obtainable is limited to

$$\theta = \pm \arcsin\left(\frac{\lambda}{2D}\right) \text{ for } D \geqslant \frac{\lambda}{2} \tag{14}$$

When $D < \lambda/2$, phase measurements are unambiguous for arrival angles within $\pm \pi/2$ of the normal to the plane containing the array faces. However, as the ratio D/λ decreases, the range of phase measurements is reduced proportionally ($\pm 2\pi D/\lambda$ for $D < \lambda/2$), hence a greater sensitivity to noise resulting in a lower angular resolution. In addition, the minimum practical spacing between the arrays is constrained by the width of each array and by the need to avoid mutual coupling effects.

To help resolve the compromise between angular resolution and phase ambiguity, additional interferometers with different array spacings can be used. For instance, mounting a third array in parallel with and at an uneven spacing from the two-array design discussed above provides three interferometers. The cost for this improvement is a requirement for three phase meters and a capability to process the three simultaneous differential phase measurements into a single angle of arrival.

In practice, the plane of the arrays is tilted 10° to 40° down from the vertical to obtain a better ensonification pattern on the bottom and to minimize ensonification of the sea surface whose returns introduce interferences in the phase measurements. This reduces the vertical separation of the arrays to $D \cos\alpha$ where α is the angle of tilt. In addition, it creates a situation where the back lobes of the arrays' radiation pattern receive signals reflected off the sea surface introducing an ambiguity in the phase measurements at the corresponding range. While designing the arrays, it is therefore necessary to control the shape of the radiation patterns to minimize the magnitude of the backlobes as well as potential sea surface ensonification with the mainlobe. Alternatively, the arrays can be baffled against sea surface returns. In practice such baffles are difficult to build as care must be taken to avoid introducing further phase ambiguities through edge diffraction effects induced by the baffle.

The foregoing phase measurement theory tends to simplify the problem of deriving bathymetry from interferometric sidescan sonars. In practice, beam patterns are not ideal and they introduce phase shifts that act as noise in the measurements. Also the seafloor is not flat and phase ambiguities result from

returns coming from more than one reflector or from a sloping bottom. These ambiguities, due to a lack of spatial correlation between the returns, have been analyzed by BLACKINTON [26] who refers to some of them as the "glissando effect" (linear frequency slide).

As the water depth increases, so does the area ensonified. The result is a decreasing spatial correlation between the returns and a wider spread in the phase measurements. Because of this, it is reportedly difficult to do swath bathymetric surveys with such systems at tow altitudes exceeding 4000 m. In power limited systems, using a long pulse length would improve the signal-to-noise ratio of the returns but correlation processing would be required to counteract the phase spread. The longer pulse length would however degrade the resolution of the concurrent side-looking sonar imagery of the seafloor.

The beam forming and beam steering operations and the conversion of differential phase measurements to acoustic angles, discussed above, all depend on the acoustic wavelength which is a function of the sound speed C, $\lambda = C/f$ with C in m/s and f in Hz. The sound speed in the ocean is a function of temperature, salinity and pressure (depth). This functionality has been expressed by MACKENZIE [27] into a nine-term sound speed equation valid for a range of temperatures between − 2° and 30° C, salinity between 30 and 40 ppt and depth to 8000 m. This equation entails that the depth, salinity and temperature dependences roughly account for a change in sound speed of respectively 1% per km, 0.075% per ppt and 0.1% to 0.3% per degree C (Fig. 2). For echo-sounding applications where the arrays remain at the same depth throughout a survey, changes in sound speed at the face of the arrays are mostly due to temperature and salinity variations, although significant salinity variations are only prevalent around estuaries. Pressure effects also come into play for towed systems operating at a fixed altitude above the bottom, and changes in sound speed at the face of the arrays can exceed 6% during surveys starting in coastal waters and extending offshore.

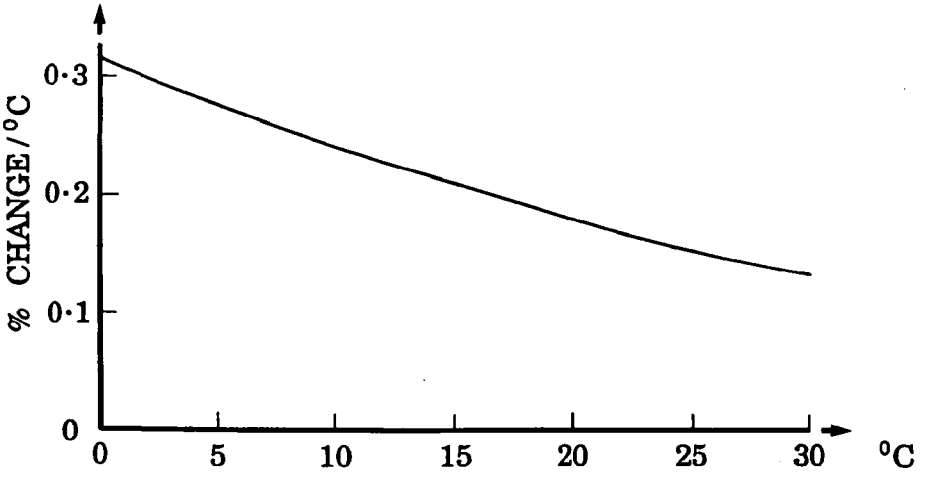

FIG. 2. — Change in the sound speed as a function of temperature in surface waters at 35 ppt salinity.

In most systems, a fixed sound speed is used to design the arrays and beam forming networks. Variations in sound speed at the face of the arrays will therefore displace the radiation pattern from its design steering direction(s). As an example, going from arctic to tropical waters (e.g. 0° to 30° C) results in a 6.6% change in the sound speed. So, for a flat array designed to produce a 2° beam, a ±3.3% change in λ changes the beam width accordingly (Eq. 8) and shifts the steering direction 3.3% to 5.7% (e.g. 1.9° at 45°) for beams steered to 60° from broadside. The corresponding error in steering angles can be corrected during echo processing using Snell's law with the design sound speed C_d and the sound speed at the face of the array C_{array} :

$$actual\ steering\ direction = arcsin\ (\sin\theta_i\ C_{array}/C_d). \tag{15}$$

Note that for conformal arrays the correction must be applied during the beamforming operation as the effect of the curvature of the array on the wave front changes with changes in the wavelength. One solution is to maintain a constant wavelength through the water by adjusting the operating frequency as a function of the speed of sound at the face of the arrays.

The variations in sound speed over the entire water column must also be taken into consideration in the swath bathymetry concept as they introduce refraction effects on oblique acoustic rays. These refraction effects limit the maximum range (swath width) achievable with a given system and failure to compensate for them produces errors in the determination of angles of arrival yielding errors in the depth and cross-track distance computations which increase with increasing angle of incidence. In correcting for refraction effects in echo-sounding, it is customary to compute the average sound speed over a ray path by integrating the sound speed profile from the depth of the array Z_{array} to the bottom Z_{max} [28]:

$$C_{avg} = \frac{1}{(Z_{max} - Z_{array})} \int_{Z_{array}}^{Z_{max}} C(z)dz. \tag{16}$$

The angle of arrival θ is then computed by applying Snell's law to the apparent angle of arrival θ_{ap} which is the sum of the actual beam steering angle (Eq. 15) and the ship's roll angle:

$$\theta = arcsin(\sin\theta_{ap}\, C_{avg}/C_{array}). \tag{17}$$

Note that in converting travel time to distance for depth calculations, the harmonic mean of the sound speed through the water column

$$C_h = \left[\frac{1}{(Z_{max} - Z_{array})} \int_{Z_{array}}^{Z_{max}} \frac{dz}{C(z)}\right]^{-1} \tag{18}$$

should be used instead of the average sound speed of Eq. (17) as it gives a more correct estimate of the sounding velocity [28].

In developing a sonar system for swath bathymetric surveys one would like to optimize the swath width capabilities as well as the range and angular resolutions of the system. Most of the parameters affecting range are contained in the simplified sonar equation which gives an estimate of the echo-to-noise ratio *EN* measurable by the system [29] :

$$EN = SL - 2TL - NL + BS + DI \tag{19}$$

where *SL* is the source level, *TL* is the transmission loss due to spherical spreading and absorption of sound waves in the ocean, *NL* is the ambient noise level in the bandwidth of the system, *BS* is the backscattering strength of the seafloor and *DI* accounts for the directivity of the transducer arrays. System noise and gains have been omitted for simplicity. Parameters not included in this equation which also affect range are the bottom relief (bottom slopes and features of scales larger than a beamwidth) and the refraction effects mentioned above.

In most systems the transmission loss is compensated automatically by applying a time-varying gain to the bottom echoes received. The backscattering strength *BS* depends on the bottom type, the angle of incidence, and the effective ensonified area (itself a function of the pulse length). As a result, the receivers need to have a dynamic range in excess of 80 dB to accommodate returns from a variety of seafloor types and at angles of incidence from 0° to over 60°.

Because absorption of sound in the ocean increases as the square of the acoustic frequency, for a given seafloor and all other parameters being held constant, absorption will condition the range capabilities of a system. As a result, acoustic frequencies between 10 and 15 kHz are typically used in systems designed for full ocean depths. Frequencies between 30 and 90 kHz are used for water depths less than 1500 m, and between 100 and 300 kHz for shallow water applications (less than 100 m).

For a given frequency, the choice of beamwidth conditions the size of the arrays (Eq. 8) which, for hull-mounted multibeam systems, also dictates their location on the hull. In practice, the preferred location for acoustic arrays on the hull of a ship is closest to the center line and as far forward as the shape of the hull permits to prevent air bubble masking [30] and reduce machinery noise effects, keeping in mind that the arrays should remain submerged throughout the ship's roll and recessed enough to prevent damage during docking operations.

Machinery noise can be further attenuated by placing an acoustic damping material in the back of the arrays a quarter of a wavelength away [31]. This also creates an image acoustic source half a wavelength from the physical array which reinforces the amplitude of the radiation pattern. Beam pattern computations for such a case are presented in the Appendix.

The problem of air bubble masking is a difficult one to predict as it depends mostly on the hydrodynamic effects created at a ship's bow which are rarely observed in modelling tanks because the Reynolds number (viscosity effects) cannot be scaled. The bubble generation process is also enhanced by protrusions, intake or vent ports near the bow as well as by bow thruster ports or tunnels. For this reason, retractable bow thrusters are better suited to hull-mounted acoustic arrays. Measurements made by the author on the Sea Beam

system installed on board the R/V *Thomas Washington* showed no noticeable increase in the noise level at the hydrophones when operating the ship's retractable bow thruster in any direction at maximum speed. On the other hand, bubble masking during a Sea Beam reception cycle in sea state 4 was found to raise the noise level by 20 to 30 dB. As a result, the performance of most hull-mounted multibeam systems degrades beyond sea state 4, particularly when heading into the seas.

Optimization of a swath bathymetric survey also depends on the ship's speed. The maximum ship's speed (v) allowable to achieve 100% coverage of the seabed in the along track direction, is a function of the sound speed C, the fore-aft width (ϕ) and the athwartships width (2θ) of the radiation pattern, as well as the slope of the bottom (α) in the across track direction (Fig. 3):

$$v = C\ tg\ (\phi/2)\ cos\ (\theta + \alpha) \tag{20}$$

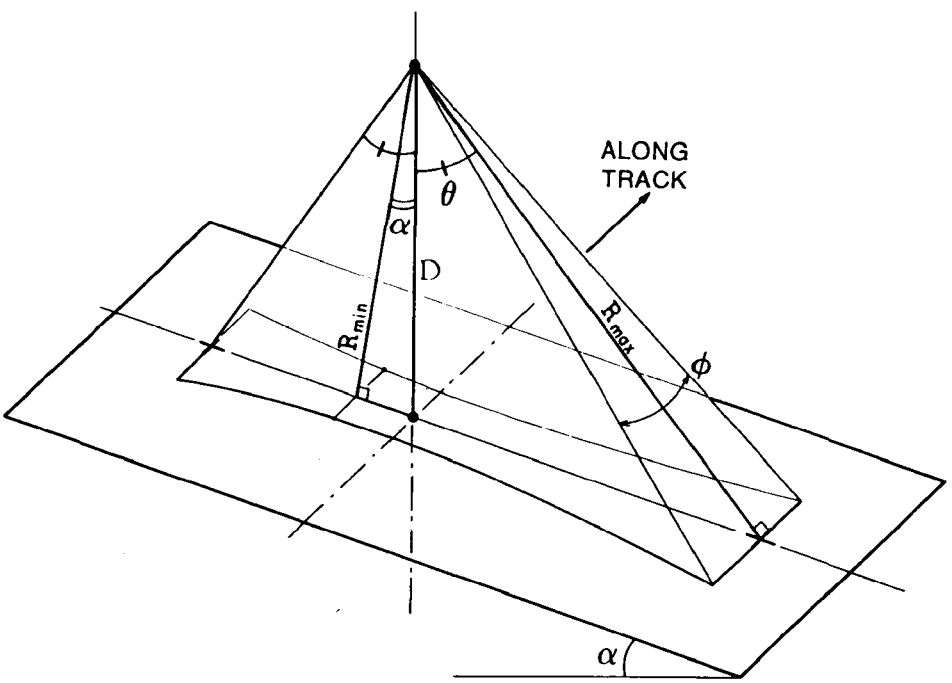

FIG. 3. — Ensonification geometry over a sloping bottom.

This function is plotted in Figure 4 for values of ϕ ranging from 0.5° to 2.66°, indicating that ship's speeds in excess of 12 knots (6 m/s) are attainable with fore-aft beamwidths 0.5° or greater for combined athwartships beam and bottom slope angles up to 45°. In practice, sea state or towing logistics condition the ship's speed and the along track coverage is routinely greater than 100%.

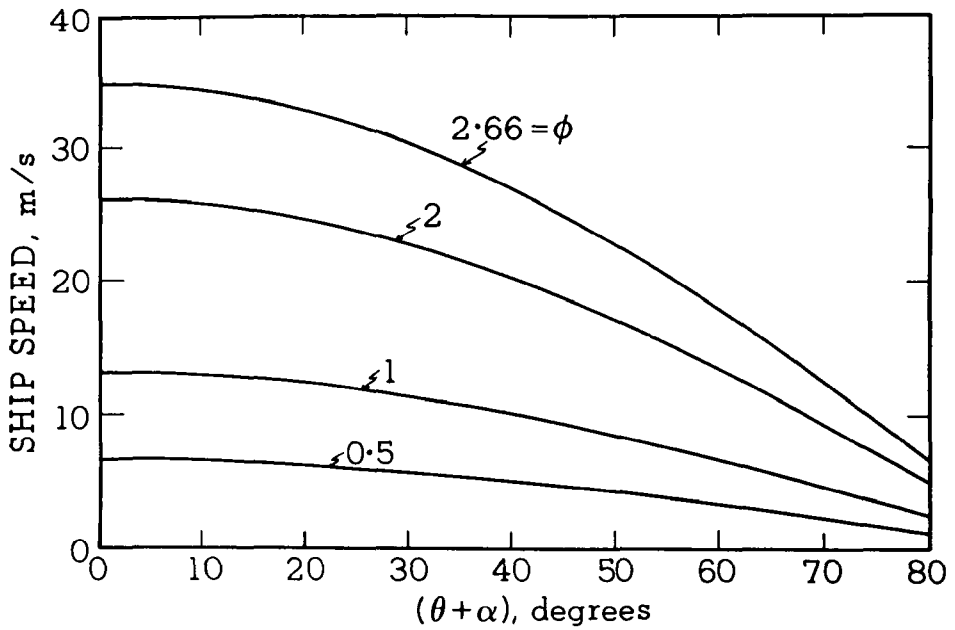

FIG. 4. — Maximum ship speed for 100% along-track coverage with narrow beam systems (Fig. 3).

3. APPLICATIONS

The theory of operation outlined above is applicable to a generic swath bathymetry system. In the following we review specific applications for several existing multi narrow beam echo-sounders and bathymetric sidescan sonars.

3.a Multibeam echo-sounders

In this section we review the characteristics of eight multibeam systems: the Sea Beam and the Hydrochart II systems manufactured in the U.S. by General Instrument Corporation, the West German systems Hydrosweep manufactured by Krupp Atlas Elektronik and Bottom Chart manufactured by Honeywell Elac, the Echos XD system manufactured in Finland by Hollming Electronics Ltd., the EM100 system manufactured in Norway by Simrad, the Multibeam Sonar System (MBSS) built by the Japan Radio Company and the towed multibeam system Benigraph manufactured in Norway by Bentech. The operating characteristics of the seven systems which use hull-mounted arrays are listed in Table 1.

These multibeam systems all follow the same general design principle based on two main components: a sonar and an echo processor. The sonar usually consists of hull-mounted transducer arrays and their associated timing unit, signal generator, power amplifiers, preamplifiers and beamforming network. The echo processor is usually a real-time computer system which is responsible for the

Table 1

Hull-mounted multi narrow beam echo-sounders: operational characteristics.

System	SEA BEAM	HYDROSWEEP	ECHOS XD		HYDROCHART II	BOTTOM CHART	EM100	MBSS
Frequency (kHz)	12.158	15.5	15	45	36	50	95	200
Projector array size (m)[1]	2.8×0.16	3×0.3	2.78×0.15	0.95×0.05	1.6×0.13	0.72×0.37	0.8×0.4	0.24
Projector beamwidth (deg.)[2]	54×2.67	90×(2.3/4.3)	4(35×2)		2(52×5)	2(60×6)	(50-120)×3	120×2
Source Level (dB/μPa/m)	230	210/220-237	220-235	220	200	230	225	197
Receiver array size (m)[1]	2.8×4	3×0.3	2.98×0.17	0.98×0.05	1.6×0.13	0.72×0.37	0.8×4	0.24
Receiver beamwidth (deg.)[2]	2.67×20	(2.3/4.3)×20	2×30		(6.3→3.5)×25	3×6	(2/2.5/5.5)×3	2x
Bandwidth (kHz)	0.225	0.3→2	0.1→1	0.2→2	0.042→1	0.3→3	5	
Sidelobe Level (dB)	25	25	25	25	25	20	23	25
Pulse Rep (sec)	1-15	1-20	4×10	4×7	0.1-4		0.25-2	0.4
Number of Beams	16	59	4×15(53 eff)		17	40	32/32/27	64
Beam Spacing (deg.)	2.67	1.5	2		6.2→3.5	3	1.25/2.5/3.75	1.8-3.5
Depth Range (m)	45-11,000	10-7,000[3]	60-6,000	6-600	10-1,500	10-1,000	10-600	
Swath Width (% water depth)	75	200	200		250	340	70/170/230	340
Roll (deg)	±20	±20 (±5)[4]	±20		±20	±20	±15	
Pitch (deg)	±10	±10	±10		±10	±10	±10	
Heave (m)		±5	±5		±10	±10	±5	
Sea State	4	4	4		4	4	5	
Ship Speed (kts)	up to 15	up to 15	up to 12		up to 15		up to 10	

[1] length × width, [2] athwartships × fore-aft, [3] to 10,000 m within ±22° incidence, [4] ±5° in calibration mode only

digitization of the echo signals received and detected on each beam, for bottom detection and tracking, for the geometric corrections (i.e. roll, heave and refraction) and the computations of depths and horizontal distances, and for the computation of depth contour plots or of waterfall plots of instantaneous depth profiles to be output to various monitors (e.g. swath plotters, graphic CRT terminals). In some systems the echo processor also includes a data logger to record the bathymetric data and the corresponding navigation. Parameters such as ship's attitude, speed and position are supplied by an external vertical reference unit (roll, pitch and heave) and by the ship's navigation system (satellite or shore based navigation and speed log).

The Sea Beam system has been in operation since 1977 and is now installed on board twelve ships worldwide: the US ships *Surveyor, T. Washington, R. Conrad, Atlantis II, Discoverer* and *Wilkes*; the German ships *Sonne* and *Polarstern*; the Japanese ships *Takuyo* and *Kaiyo*; the French ship *J. Charcot* and the Australian ship *HMAS Cook*. Its operation and performance have been well documented in the literature [13, 32, 33] and are only briefly outlined here. The projector array is made of 20 units aligned along the keel, and the hydrophone array which consists of 40 units is mounted athwartships and centered on the keel. To accommodate various hull shapes, the hydrophone array can be conformed into a V shape with up to 15° of inclination from the horizontal (Appendix). Phase steering, as described in Section 2, is used to ensure vertical projection on transmit, and 16 beams are formed through a resistor matrix with four quadrature inputs for each of the 40 preamplifiers. A Dolph-Chebyschev shading function effectively reduces the sidelobes on the transmit and the receive beam patterns roughly 25 dB below the mainlobe. After corrections for roll and refraction effects, the depth on each beam is determined by calculating the center of mass of the echo signal exceeding a dynamic threshold and contained within a reception window.

Because the swath width of the Sea Beam system is roughly 3/4 of the water depth, the system is marginally useful in shallow water. GIC designed the Hydrochart II system [34] to fill this need. This system is the latest revision to a shallow water multibeam echo-sounder built by GIC. The original sonar system, called BO'SUN [31, 35], is a 21 beam system operating at 36 kHz with 5° beams for a total swath width of 2.5 times the water depth and a 600 m depth capability. The BO'SUN uses two identical pairs of projector and hydrophone arrays. Each pair is oriented to port and starboard respectively and performs a transmit receive cycle on alternate ping cycles, thus forming 11 beams to each side with 1 beam overlap in the vertical. This technique provides a wide ensonification pattern athwartships with narrower preformed beams and requires less power and smaller arrays than would a single array pair with similar overall coverage. After solving a number of acoustic problems related to the arrays' installation, addition of real-time displays, data acquisition and processing systems as well as a Datawell Hippy 120 vertical reference unit, the sonar system was turned into the Bathymetric Swath Survey System (BSSS) installed on the NOAA ship *Davidson* [36, 37]. The BSSS system is also referred to as Hydrochart by GIC [13].

The Hydrochart II system incorporates the various external sensor inputs available to the BSSS into a modular design, but it differs from its predecessors in

its sonar geometry and depth capability. The pairs of projector and hydrophone arrays are housed in separate domes on port and starboard, and the plane of each array pair is tilted 25° from horizontal. Nine beams are formed to each side with one beam overlap in the vertical. The particularity of this system is a beamwidth decreasing from 6.3° in the center to 3.5° for the outer beam, yielding an approximately constant footprint on the seafloor, hence more uniform depth measurements across all beams. The depth capability of the system has also been increased to 1500 m (2000 m for high backscatter seafloors) which makes it suitable for most coastal waters and Continental Shelf surveys. The system has been operational on the Japanese vessel *Tenyo* since March 1987, and it is scheduled to replace the BSSS on the *Davidson*.

The Hydrosweep system was designed and built to provide swath bathymetry mapping capabilities for the new German research vessel *Meteor* delivered in 1985. This system expands on the Sea Beam design by providing a wider swath width (twice the water depth) with 59 beams. It uses two identical arrays mounted at right angles to each other, one of them being parallel to the ship's keel. Each array is made up of three modules of 96 elements arranged in a planar configuration with 4 rows of 24 elements. Because they are identical, these arrays can be used either in transmit mode by driving each element separately, or in receive mode by combining the elements in groups of 4 to form 72 receive channels. These 72 channels are used to form 59 beams spaced 1.5° apart with beam widths ranging from approximately 1.9° in the center to 2.7° for the outer beams (Eq. 8). Depending on which array is used as a projector, the transmitted beam is stabilized against roll or pitch. Beamforming is done through digital time delay lines and a modified $\cos^2$ window maintains the sidelobes roughly 25 dB below the mainlobe.

By design, the arrays must remain flat, and given their length (3 m), it is necessary to mount them toward the ship's midsection where the hull is least curved. As discussed in Section 2, this type of installation is prone to air bubble masking. On the *Meteor* the situation was aggravated by a bulbous bow whose associated bow wave and trough siphoned air bubbles along the ship's bottom and almost completely hampered acoustic measurements for ship speeds between 2 and 10 knots [30]. The problem was solved in a drastic manner by eliminating the bulb.

Taking advantage of the interchangeability of the transmit and receive functions between the two arrays, the system enters a 'calibration' mode by switching from the standard athwartships receive pattern to a fore-aft receive pattern every 25 pings. By comparing the depth measurements made on the center beam in the athwartships mode over a number of successive pings with those obtained on the 59 beams in the fore-aft mode, the system is able to perform an approximate raybending inversion and to determine the mean sound speed through the water column which is then used for subsequent refraction corrections. As discussed in Section 2, the value of the sound speed at the array's face is also used in the refraction corrections. In the Hydrosweep system this value is measured by a sound velocimeter using a 210 kHz transducer mounted on the hull at the same draft as the arrays.

After compensating for refraction and roll, the echo processor computes the

depth on each beam at the arrival time corresponding to the mean of the echo amplitudes exceeding a noise threshold in the reception window. To overcome jitter in the depth data due to beam overlaps, the depth values given by the echo processor are smoothed over three consecutive pings by replacing each datum with the weighted average of itself and its eight immediate neighbors. These smoothed depth data are then contoured for on-line displays as well as stored by a data logger.

A menu driven display allows the operator to check the performance of the system in real time and to control the data output and presentation formats to a variety of monitors. The real-time checks include a display of the reception window, the position and number of valid beams for each ping cycle, as well as the cumulative echo level and gain settings on 8 beams selected by the operator.

In addition, the Hydrosweep system can operate in one of four modes. (1) a shallow mode for water depths between 10 and 80 m in which only half of the arrays are used to transmit a 0.5 msec pulse of 15.5 kHz and receive beams are approximately 4.3° wide. (2) an intermediate mode for depths to 1000 m where only one line of 72 elements is used to transmit a 1 msec pulse and the whole receive array is used to form beams about 1.9° to 2.7° wide from center out (average 2.3° given in Table 1). Modes 3 and 4 differ from the two preceding ones in the transmit geometry used. To provide a more uniform ensonification pattern over the 90° athwartship sector, a transmit beam 45° wide athwartships is step scanned in three directions, the first one centered on the vertical and the other two centered at ±22.5° incidence. The time elapsed between each step is less than 0.6 msec. This method is referred to as sectoral directional transmission (SDT) by the manufacturer. In mode 3, the pulse length is limited to 2 msec for depths to 2000 m. In mode 4, the pulse length is 5 msec for the sector centered on the vertical and 11 to 16 msec for the two other sectors. In this mode, depth to 10,000 m are measurable on a subset of the 59 preformed beams contained within ±22° of the vertical. Depths between 5,000 and 7,000 m can be measured on the full ±45° span of the 59 beams depending on the acoustic backscattering characteristics of the seafloor surveyed.

Whereas GIC addresses the deep vs shallow water swath mapping problem by providing two different systems, the Krupp Atlas design combines both capabilities in a single frequency system. By contrast, the Echos XD is a dual frequency systems, 15 kHz for depths to 6,000 m and 45 kHz for depths to 600 m, with separate array pairs for each frequency. This 60 beam echo-sounder is an evolution of an earlier 15 beam system, similar in concept to the Sea Beam system, that was developed in the early 1980's and installed on three ships from the USSR Academy of Sciences: *Akademik Nikolaj Strakhov, Boris Petrov* and *M.A. Lavrentyev*. Note that two of these ships were originally built with bulbous bows which had to be removed because of bubble masking problems akin to those described for the R/V *Meteor*. The new system is installed on the *Akademik Sergej Vaviloff*, a new Russian ship delivered in December 1987, and a second installation is planned on a sister ship to be delivered in December 1988.

The originality of the Echos XD design lies in its transmit-receive geometry. Each array contains 57 elements arranged in a planar configuration with 3 rows of 19 elements. All 57 elements are used on receive and a subset (35 elements) is

used for transmit. To obtain a swath width comparable to that of the Hydrosweep system (roughly twice the water depth), a set of 15 2° beams is scanned in 4 angular sectors on successive pings with a 10 sec ping rate. The transmit beam must therefore be stabilized in both pitch and roll. The transmit sequence starts with the transmit beam (40° by 2°) centered at −30° incidence. On the next ping, it is centered at −10° incidence, followed by +30° and +10° before repeating the sequence. As this ensonification pattern creates some overlaps, the effective number of beams across the swath is 53.

Beamforming is done through analog delay lines and sidelobe reduction roughly 25 dB below the mainlobe is obtained with a generalized Hamming window. A processing subsystem handles the bathymetric data, the ship's navigation and attitude information and controls outputs to all the peripherals (i.e. monitors, magnetic tape recorders, graphic recorders) through a Local Area Network (LAN). The operator accesses this subsystem via a menu driven console. Unlike the other multibeam system reviewed here, the Echos XD presents the user with the possibility to record either the raw acoustic data for each beam, along with a time reference and pitch and roll information, or the processed depth data along with navigation, pitch, roll and the man sound velocity used in the depth computation. A capability to preserve the raw acoustic data is very useful if one wants to verify the performance of the system [33] or to extract information from the echo signals in addition to the bathymetry (e.g. seafloor acoustic backscatter characteristics, acoustic imagery) [38, 39]. The system has built-in provisions to record simultaneously the bathymetric data and the acoustic data, however this requires reducing the ping rate.

The Bottom Chart system [40] is a new design which uses a transmit-receive geometry similar to that of the Hydrochart II system but with constant beam widths. Instead of array pairs on either side of the ship, this system uses one 28 elements array per side. Each array is included 30° from the horizontal and is used for both transmit and receive functions. Twenty adjacent beams roughly 3° wide athwartships are formed on each side. The resulting coverage is about 120° yielding a swath width roughly equal to 3.4 times the water depth. As with the Hydrosweep system, some form of on-line adaptive raybending correction is implemented in this system, however it is imbedded in a proprietary algorithm. This system also offers the possibility to record simultaneously the raw and processed data for post-processing applications. The only system in operation at this time is installed on the company's vessel *Poseidon*.

The next two echo-sounders are designed for mid to shallow water work. The EM100 system [41] was developed in response to survey needs in fjords, and it was first installed in April 1986 on the survey vessel *Geofjord* owned by the Norwegian survey company Geoconsult A/S. Geoconsult has since acquired a second system, and systems are installed on the Norwegian hydrographic vessel *Lance* as well as on a clamshell trawler. Two more systems are installed on Simrad's vessels *Simson Echo* and *M/K Simrad*. The particularity of this system is that it transmits and receives with a single array which is mechanically stabilized against pitch. The array is retractable in the hull and extends about 80 cm below the hull in its operational position, thereby avoiding most of the bubble masking problems encountered on the hull. Such a design is made possible by the small array size (< 1 m) required at the operating frequency of 95 kHz. The

array is curved through a 120° arc with a radius of 45 cm and is made up of 96 elements. On receive, a symmetrical combination of 16, 32 or 40 elements is used to form beams whose steering direction is always perpendicular to the face of the array at the mid point of the element combination. The beamforming is done digitally allowing a choice of beamwidths and beam spacing depending on the survey requirements and on the acoustic backscattering characteristics of the seafloor surveyed. Three modes are available: a narrow mode with 32 2° beams with 1.25° spacing (swath width of 0.73 × depth); a wide mode with 32 2.5° beams with 2.5° spacing (swath width of 1.7 × depth) and an ultra wide mode with 27 5.5° beams with 3.75° spacing (swath width of 2.3 × depth).

A PC with a custom 16-bit bitslice processor serves as echo processor, beam former and sonar timing unit. The echo processor uses a combination of envelope detection and interferometric processing to determine the arrival time of bottom returns within a dynamic bottom tracking window. A menu driven operator's console provides system performance checking and peripherals control capabilities similar to those described for the other systems. As with the Hydrosweep display, the instantaneous depth profile across track is displayed with an echo amplitude histogram for all 32 beams. It is also possible to display a depth profile along track for a specified beam, including a histogram of the echo amplitude received on this beam at each ping cycle.

With an operating frequency of 200 kHz, the MBSS system is confined to shallow water surveys in harbors, rivers and shallow coastal areas [42, 43]. This system differs from those discussed above by using a complex fast Fourier transform (CFFT) beamformer to produce 64 beams within ± 60° of the vertical, with beamwidths of roughly 2° in the near vertical and increasing with the angle of incidence (Eq. 8, 12). Amplitude shading with a Hanning window ($\cos^2$) effectively lowers the sidelobes 25 dB below the main lobe.

At 200 kHz and in shallow water, echoes returned by volume scatterers (mostly suspended sediment) interfere with the bottom detection process as their amplitudes are comparable to that of the bottom echoes. For a random distribution of scatterers in the volume, it is fair to assume that the resulting echoes are uncorrelated from one ping to the next. By further assuming that some correlation is retained by the bottom returns over a few pings, a condition approximated when the ship's speed is such that substantial overlap occurs between pings, the bottom detection is improved by averaging the echoes received over a few pings. In the MBSS an average of 4 to 8 pings is used depending on the ship's speed and the acoustic backscattering properties of the bottom.

All the multibeam echo-sounders listed in Table 1 operate with hull-mounted arrays mostly because the cross fan beams geometry requires large arrays that would be difficult to install in an L or a T configuration on a towable vehicle. However, for operating frequencies in excess of 100 kHz, the arrays are small enough to be mounted on a conventional towed vehicle as was done for the Benigraph system manufactured by Bentech in Norway [44]. This system operates at 740 kHz with possibilities to select two alternate frequencies: 1 MHz and 515 kHz. The receive array consists of 256 elements whose outputs are quadrature sampled and multiplexed into an analog beamformer. The beamformer uses the Chirp Z-transform [45], and the surface acoustic waves technology found in radar

applications to form 200 beams with an angular resolution of 0.75° (0.5° at 1 MHz and 1° at 515 kHz respectively) and a 90° cross-track coverage (200% of the vehicle's altitude). Signals received on each beam are then envelope detected, digitized and sent up the cable to the echo processing system on board ship. The tow cable is a hybrid double-armored cable with fiber optics conductors for data transmission and copper conductors for power and signal transmissions. The vehicle is roughly 4 m long by 0.8 m in diameter and contains the sonar electronics, an inertial navigation system for attitude and heading and an acoustic positioning system to track tow depth and position behind the ship. The vehicle is towed 10 to 40 m above the bottom in water depth to 300 m, at tow speeds up to 7 knots. Although the swath width obtained in these conditions is on the order of 60 m or less, the 0.75° angular resolution and a range resolution better than 0.1 m allow for very detailed surveys, as required for submarine pipeline inspection work.

For shallow water work in harbors, rivers and estuaries, multi transducer boom systems offer a low cost alternative to the more sophisticated multi narrow beam echo-sounders described above. An example of such systems is the Echoscan multi transducer survey system manufactured by Odom Hydrographic Systems. In this design, up to 32 transducers operating at 200 kHz with 16.8° beamwidths are evenly spaced on a boom which is either secured alongside a barge or towed in front of a small survey vessel. The transducer spacing is adjustable, depending on the water depth, to provide optimum bottom coverage with minimal overlap between beams from adjacent transducers. Each transducer operates as a separate channel and no beamforming is performed.

3.b Bathymetric sidescan sonars

Even when the operating acoustic frequency is high enough to install a multi narrow beam system in a tow body, such a system remains relatively complex, hence costly, and with limited swath width capabilities. By comparison, towed bathymetric sidescan sonars are conceptually simpler and cheaper to build, and they offer a wider bathymetric coverage, although with less accuracy, in addition to conventional side-looking sonar imagery of the seafloor. Also, they can be operated from ships of opportunity adding flexibility and cost effectiveness to a bathymetric survey plan. Table 2 summarizes the characteristics of three such sidescan systems ordered by increasing acoustic frequency: SeaMARC II (HIG), SeaMARC/S (SSI) and Bathyscan which is built and operated by Bathymetrics Ltd. In the following, we confine ourselves to the bathymetric aspect of these systems.

The two SeaMARC systems have the same basic architecture [22, 23, 26]. Arrays are mounted on each side of a neutrally buoyant tow vehicle with their long axis parallel to the direction of tow. This vehicle is designed with a large righting moment to minimize its roll which would otherwise disrupt the phase measurements. To minimize heave and pitch in the vehicle, a depressor and a neutrally buoyant tether link the vehicle to the tow cable. In addition, a bridle and drogue combination attached to the stern of the vehicle acts as a passive stabi-

Table 2

Bathymetric sidescan sonars: operational characteristics

System		SeaMARC II	SeaMARC/S	Bathyscan
Frequency (kHz)		P11,S12	150	300
Bandwidth (kHz)		2→0.1	50→3	50
Array Size (m)[1]		3.8×0.2	0.5×0.1	
Beamwidth (deg)[2]		2×40	1×50	1×50
Source Level (dB/μPa/m)			220	220
Transmission rate (sec)		1,2,4,8,16	0.05→1	0.2
Fish Size (m)[3]		5.5×1.3	2×0.4	2×0.4
Tow	depth (m)	1-1000	1-1,500	2-100
	altitude (m)	up to 10,000	2-500	30-60
	speed (kts)	up to 10	up to 6	up to 7
Depth Range (m)		10-6,000	3-2,000	5-150
Swath Width (% tow altitude)		340	340	700

[1] length × width, [2] fore-aft × athwartships, [3] fore-aft atwartships

lizer to further reduce the vehicle's pitch and yaw. Roll, pitch and yaw are also measured inside the vehicle and used to correct the data during post-processing operations.

In the SeaMARC II, each side has a pair of identical arrays, with roughly $\lambda/2$ spacing for interferometry. The arrays in each pair transmit in parallel and receive independently. For each pair the complex acoustic signals received (I,Q) are sampled at 4 kHz. In the SeaMARC/S, three arrays are used on each side with 1 and 2 λ spacing between them. One of them is used only to transmit, and the two others form a 1 λ interferometer and receive independently. In the current design, only one interferometer out of the possible three is used, and the phase data occupy two phase circles. The sampling rate for each pair of receivers is 100 kHz.

If the ratio of the magnitudes of the phase data measured at the two arrays in each pair is close to 1 (within ±15%), the phase data are considered valid and are entered into a two-dimensional histogram of phase angle vs time. To minimize the phase ambiguities due to lack of coherence of the signals between the two arrays (Section 2), a ridge following technique is used to extract a relatively smooth curve of phase angle as a function of time [46]. This curve is then translated into acoustic angles of arrival as a function of time via table look-up. The conversion table is established empirically by 'calibrating' the system over a flat seafloor. Note that such a calibration method incorporates the raybending effects and must therefore be rerun before each survey or whenever the sound velocity profile changes.

Both SeaMARC systems have a swath width of approximately 340% of the tow altitude (roughly ±60° incidence). In SeaMARC II, this corresponds to the onset of the first bottom multiple (vehicle-bottom-surface-bottom-vehicle) which reaches the arrays at the same time as bottom returns from angles of incidence greater than 60° and creates an interference in the phase data. For a tow depth T and a water depth D, the angle of incidence γ at which bottom returns and the

first bottom multiple coincide is given by:

$$\gamma = arccos\left(\frac{D-T}{2D-T}\right) \tag{21}$$

For shallow water surveys, or for systems like the SeaMARC/S which are constrained to a maximum altitude above the bottom, the onset of the first bottom multiple will usually take place beyond the 60° incidence angle. Note that provided the source level of the system is sufficient to retain a workable signal-to-noise ratio past the first bottom multiple, bathymetry data can be recovered beyond the interference; however, because the area ensonified increases with the angle of incidence, the corresponding phase data is affected by the phase spread problem mentioned in Section 2. In addition, the interference from the first bottom multiple could be reduced by adaptively steering a null in the beam pattern in the direction of the interference.

About 50 sounding points per side are obtained every ping with the SeaMARC II system and a color coded bathymetric swath with roughly 50 m contour resolution is output in real time in addition to the conventional range corrected sidescan imagery of the seafloor. With the SeaMARC/S system, about 128 sounding points per side are displayed in a similar fashion at 1 to 5 m contour resolution.

The Topo-SSS design [21] illustrates the limitations on unambiguous phase measurements due to the width and spacing of the arrays (Eq. 14). This system was an experimental design whose development has been discontinued (F. PØHNER, personal communication). The transducer arrays are approximately 1.8 λ in width and the spacing between their centers is 1.9 λ. As a result, phase can only be measured unambiguously within $\pm 15°$ of the normal to the plane of the arrays. The plane of the array is tilted 20° from the vertical and a swath roughly twice the tow altitude in width and offset from the tow track by about 1.4 times the tow altitude is obtainable on either side. Although the geometry could provide a swath width of roughly 10 times the tow altitude for each side, signal coherence degrades with increasing range resulting in noisy bathymetry. In this system, the interference from the first bottom multiple is strongly attenuated by the beam pattern and comes in at the edge of the angular sector in which phase measurements are unambiguous. To compensate for the vehicle's roll imparted by a direct connection to the tow cable, a roll correction is applied to the phase measurements in real time before converting to bathymetry.

To overcome the limitations illustrated with the Topo-SSS experimental design, the Bathyscan system [19, 20, 47] uses three parallel arrays unevenly spaced but, unlike the SeaMARC/S design, two interferometers with different phase ramps are formed. Only one of the arrays is used to transmit. The original version of this system, built at Bath University (U.K.), used interferometers with 13 and 14 λ spacings [18]. By subtracting one phase ramp from the other, a 1 λ vernier is obtained allowing resolution of phase ambiguities that would occur with a single interferometer. In its current configuration, the Bathyscan system uses the same geometry but the interferometers are on the order of 10 λ, and the arrays are inclined roughly 20° from vertical. Further phase ambiguity resolution is achieved by cross-correlation between the two phase difference measurements. The correlation must exceed a preset threshold (typically 0.85) for the data to be

accepted, however, the correlation is also a function of the signal-to-noise ratio in the measurement and the threshold must be lowered in areas of low acoustic backscatter.

This system transmits alternately on port and starboard. Approximately 2000 phase angles are recorded for every ping. These angles are used to compute 200 depth points spaced about 0.5 m apart, for a range to one side of 100 m. On sandy bottoms, the acoustic backscattering characteristics of the bottoms make it possible to obtain ranges of 150 m to one side, in which case 300 depth points per side are recorded (R.L. CLOET, personal communication). In order to obtain soundings with roughly the same spacing along and across track (0.5 m), the tow speed should be approximately 5 knots. It is however possible to tow the fish at up to 10 knots. The fish is usually towed 30 to 60 m above the bottom and bathymetric swaths 7 times the tow altitude in width are routinely obtained. Real-time displays include stacked cross-track bottom profiles plots and data density (bottom coverage) plots. In this system, the bulk of the phase data processing is done off-line because of the computational burden imposed by the need to reconcile the measurements from the two interferometers and the necessity to rid the data of echoes from volume scatterers as discussed above for the MBSS system.

4. CONCLUSION

In reviewing the design characteristics of swath bathymetry systems, we have seen that the technology of multi narrow beam echo-sounders ushered in the non-military world with GIC's Sea Beam system is maturing with new developments offered in the last five years by several non US companies (e.g. Bentech, Hollming Ltd., Honeywell Elac, Krupp Atlas, Simrad). In addition to some innovative design concepts, some of these new systems have started to improve on the beam formation process by taking advantage of the increasing availability of integrated digital signal processing technology. The new systems claim swath widths of up to twice the water depth (up to 3.4 times the water depth for shallow water applications) with depth and angular resolutions comparable to those of the Sea Beam system whose swath width is limited to 3/4 of the water depth. However, these systems have not been extensively tested over a variety of seafloor terrains and their overall performance remains to be determined.

One of the weak points of the multibeam echo-sounder technology is the rather empirical positioning of the acoustic arrays on the ship's hull. The best electronic and echo processing designs can be rendered useless if sound cannot reach the bottom or be received at the hydrophones because of air bubble masking. The installation of acoustic arrays over 3 m in length should be integrated in the hull design process as much as possible and, for new installations on existing ships, a careful noise and bubble masking trial at sea should be conducted before the installation.

Interferometric sidescan sonars offer the advantage of transportability, simpler

design requirements and swath widths of up to 7 times the sonar's tow altitude over the bottom with concurrent sidescan acoustic imagery of the seafloor. Although the bathymetry currently obtainable with these systems is of lower accuracy than their multi narrow beam counterpart, improvements in phase processing and interference rejection should enhance both the angular resolution and the swath width.

In the future, the compromise between high resolution bathymetry and wide coverage might be reached by combining the multi narrow beam and the interferometric technologies into a towed hybrid system for use in shallow water and in the open ocean by towing a bathymetric sidescan sonar behind a ship equipped with a hull-mounted multi narrow beam echo-sounder. In both cases, seafloor trends unveiled by the multibeam sounder in the center portion of the swath could be followed in the sidescan bathymetry, thereby optimizing the survey pattern and reducing the guess work for interpolating between survey lines.

ACKNOWLEDGMENTS

I wish to thank D.E. PRYOR (NOAA/NOS/CGX3) for reviewing this paper and providing many helpful comments and corrections. I also thank D. ALEXANDROU (Duke Univ.) and J.G. BLACKINTON (SSI) for their comments on the manuscript; V.C. ANDERSON and W.S. HODGKISS (MPL) for their advice. For providing information and review comments on the systems described in this paper, I am indebted to W. CAPELL and S. WITHROW (GIC), E. EROLA and T.P. JÄNTTI (Hollming Ltd.), R. ZIESE and R. SCHREIBER (Krupp Atlas Elektronik), F. PØHNER (Simrad) and R.L. CLOET (Bathymetrics Ltd). I am also indebted to J. GRIFFITH who drafted the figures and E. FORD for editorial help.

APPENDIX

Calculations involving planar arrays

To illustrate the beam pattern calculation for planar arrays, we consider the case of an array of 2N point sources shaped as a Sea Beam receiver array into a V with an inclination angle Ψ from the horizontal and an acoustic image half a wavelength away (Fig. 5). Placing the origin of coordinates at the center of the physical array enables us to define each point source location, in the $y = 0$ plane, by its (x,z) coordinates and the direction cosines ($l \equiv \cos \alpha$, $m \equiv \cos \beta$, $n \equiv \cos \gamma$) of the wave front vector to that point (Fig. 6). Taking the origin 0 as the origin of phase, each point source C(x,0,z) is out of phase with 0 by the amount $e^{jk(xl+zn)}$ which uses the scalar product of the vector OC(x,0,z) and the wave front vector with direction cosines (l,m,n). It follows that a wave traveling in the direction (l,m,n) produces a pressure field over the 2N elements of the array:

$$P = \sum_i A_i \, e^{jk(x_i l + z_i n)} \qquad (22)$$

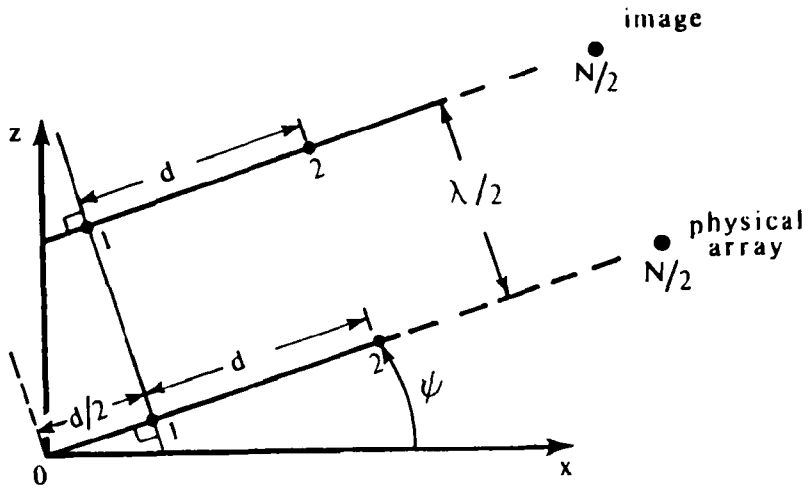

FIG. 5. — Geometry of a V-shaped array with 2N elements and an acoustic image a half wavelength away.

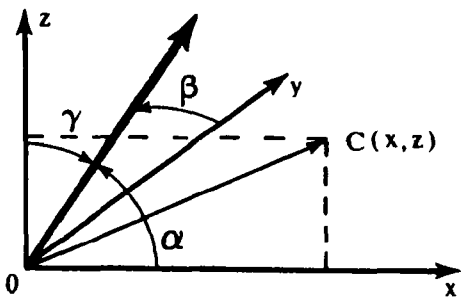

FIG. 6. — Direction cosines.

where A_i is the amplitude at element i (the time dependence has been omitted for simplicity).

The resulting radiation pattern is obtained by summing real and imaginary parts separately and calculating the magnitude of Eq. (22).

$$P = [\mathrm{Re}^2\{P\} + \mathrm{Im}^2\{P\}]^{1/2} \tag{23}$$

Coordinates of points in the physical array and its image

As shown in Figure 5, the elements of the array are numbered from the origin out for both the physical array and its image. In the physical array, (subscript P) the coordinates of the i^{th} element from the origin are:

$$x_{iP} = \frac{(2i-1)}{2} d \cos \Psi \text{ and } z_{iP} = \frac{(2i-1)}{2} d \sin \Psi \tag{24}$$

where d is the element spacing.

For the image, the i^{th} image element has coordinates (subscript I)

$$x_{iI} = 1/2((2i-1)\ d \cos \Psi - \lambda \sin \Psi)$$
$$\text{and } z_{iI} = 1/2((2i-1)\ d \sin \Psi + \lambda \cos \Psi) \tag{25}$$

The direction cosines are written as a function of the polar angle θ and the azimuthal angle ϕ in the form:

$$\begin{aligned} l &= \sin\theta \cos\phi \\ m &= \sin\theta \sin\phi \\ n &= \cos\theta \end{aligned} \tag{26}$$

combining Eq. (24-26) into Eq. (22) yields the radiation pattern for the physical array and its image:

$$P(\theta, \phi) = \sum_{i=1}^{N} A_i e^{jk(x_{iP} \sin\theta \cos\phi + z_{iP} \cos\theta)} + \sum_{i=1}^{N} A_i e^{jk(x_{iI} \sin\theta \cos\phi + z_{iI} \cos\theta)} \tag{27}$$

Since the array is symmetrical with respect to the Z axis, Eq. (27) simplifies into:

$$P(\theta, \phi) = \sum_{i=1}^{N/2} A_i\ e^{jkz_{iP} \cos\theta} 2 \cos(kx_{iP} \sin\theta \cos\phi) +$$
$$\sum_{i=1}^{N/2} A_i\ e^{jkz_{iI} \cos\theta} 2 \cos(kx_{iI} \sin\theta \cos\phi) \tag{28}$$

which when normalized to its on axis value ($\theta = 0$) yields:

$$P(\theta, \phi) = \left[\sum_{i=1}^{N/2} A_i\ e^{jkz_{iP}}(1 + e^{j\pi \cos\Psi})\right]^{-1}$$
$$\left[\sum_{i=1}^{N/2} A_i\ e^{jkz_{iP} \cos\theta} \cos(K\, x_{iP}) + \sum_{i=1}^{N/2} A_i\ e^{jkz_{iI} \cos\theta} \cos(K\, x_{iI})\right] \tag{29}$$

$$\textit{where } K = k \sin\theta \cos\phi$$

Radiation pattern of an ideal Sea Beam receive array

Assuming each element of the array is a cylindrical hydrophone of length L along the y axis and approximating the pattern of the circular section in the x, z plane by that of a point source, we use the pattern multiplication theorem to determine the radiation pattern of the whole array.

For a continuous line source of length L, the radiation pattern is:

$$P_L(\theta) = \frac{\sin Y}{Y} \text{ where } Y = \frac{\pi L}{\lambda} \sin\theta \tag{30}$$

thus, after multiplication by Eq. (29), the radiation pattern of the array is:

$$P(\theta, \phi) = \frac{\sin Y}{Y}\left[\sum_{i=1}^{N/2} A_i\, e^{jkz_{iP}}(1 + e^{j\pi\cos\Psi})\right]^{-1}$$

$$\left[\sum_{i=1}^{N/2} A_i\, e^{jkz_{iP}\cos\theta}\cos(K\,x_{iP}) + \sum_{i=1}^{N/2} A_i\, e^{jkz_{il}\cos\theta}\cos(K\,x_{il})\right] \tag{31}$$

$$\text{with } Y = \frac{\pi L}{\lambda}\sin\theta \text{ and } K = k\sin\theta\cos\phi$$

This function is plotted in Figure 1 in the text for $\phi = 0°$ and $\Psi = 10°$.

Beam steering

In order to generate a preformed beam in a particular direction, one has to phase the signals from all the hydrophones so that they all reach the corresponding receiver simultaneously. In the Sea Beam receiver, preformed beams are spaced 2 2/3° apart so that θ varies from 1 1/3° to 20° by steps of 2 2/3°, for a total of 8 preformed beams on either side of the vertical.

For a preformed beam in the direction (l', m', n'), it is convenient to correct the contributions of each element for phase by bringing them to a common reference plane, parallel to the wave front plane, and passing through the origin 0 which we defined as the origin of phase. The pressure field over the 2N elements of the array given in Eq. (22) is then modified by the corresponding phase correction:

$$\sum_i A_i\, e^{jk(x_i l + z_i n + x_i l' + z_i n')} \tag{32}$$

or in terms of the polar angle θ, the azimuthal angle ϕ and the preformed beam direction θ', ϕ':

$$P(\theta, \phi) = 2\sum_{i=1}^{N/2} A_i\, e^{jK_z z_{iP}}\cos(K_x x_{iP}) + 2\sum_{i=1}^{N/2} A_i\, e^{jK_z z_{il}}\cos(K_x x_{il})$$

$$\text{with } K_x = k(\sin\theta\cos\phi + \sin\theta'\cos\phi') \tag{33}$$

$$K_z = k(\cos\theta + \cos\theta')$$

References

[1] HAINES, G.: (Chapters 3 and 5), in *Sound underwater*, 1974, Crane Russak, New York, N.Y.

[2] TUCKER, D.G. and J.G. HENDERSON: Automatic stabilization of underwater acoustic beams without mechanical motion of the transducer, *Int. Hydr. Rev.*, vol. 37(1), 1960, pp. 69-78.

[3] TUCKER, D.G.: Directional echo-sounding, *Int. Hydr. Rev.*, vol. 37 (2), 1960, pp. 43-53.

[4] FARENTHOLZ, S: Profile and area echograph for surveying and location of obstacles in waterways, *Int. Hydr. Rev.*, vol. 40(1), 1963, pp. 23-37.

[5] ENGELMANN, I.: Towed echosounders for parallel sounding, *Int. Hydr. Rev.*, vol. 44(2), 1967, pp. 7-10.

[6] STENBORG, E.: The Swedish parallel sounding method — State of the art, *Int. Hydr. Rev.*, vol. 64(1), 1987, pp. 7-14.

[7] DINN, D.F., R.G. BURKE, G.D. STEEVES, and A.D. PARSONS: Hydrographic instrumentation and software for the remotely controlled survey vehicle 'Dolphin', *Proc. IEEE/MTS Oceans'87 Conf.*, vol. 2, 1987, pp. 601-607.

[8] HOWSON, E.A. and J.R. DUNN, Directional echo-sounding, *J. Inst. of Navigation*, vol. 14, 1961, pp. 348-359.

[9] TUCKER, M.J.: Beam identification in multi-beam echo-sounders, *Int. Hydr. Rev.*, vol. 38(2), 1961, pp. 25-32.

[10] GLENN, M.F.: Introducing an operational multi-beam array sonar, *Int. Hydr. Rev.*, vol. 47(1), 1970, pp. 35-39.

[11] PHILLIPS, J.D. and A.S. FLEMING: Multibeam sonar study of the MAR Rift Valley 36-37°N, Map Series MC-19, *Geol. Soc. of Amer.*, 1978, Boulder, Colo.

[12] GLENN, M.F.: Multi-narrow beam sonar systems, *Proc. MTS-IEEE Oceans'76 Conf.*, 1976, pp. 8D-1 - 8D-2.

[13] FARR, H.K.: Multibeam bathymetric sonar: Sea Beam and Hydrochart, *Marine Geodesy*, vol. 4 (2), 1980, pp. 77-93.

[14] NICKLES, J.C. and V.C. ANDERSON: Vertical obstacle sonar prototype trials, *JASA (76th meeting of ASA, Nov. 1968)*, vol. 45(1), p. 306.

[15] STUBBS, A.R., B.S. McCARTNEY, and J.G. LEGG: Telesounding, a method of wide swathe depth measurement, *Int. Hydr. Rev.*, vol. 51(1), 1974, pp. 23-59.

[16] KOLOUCH, D.: Interferometric side-scan sonar, a topographic sea-floor mapping system, *Int. Hydr. Rev.*, vol. 61(2), 1984, pp. 35-49.

[17] DENBIGH, P.N.: Phase only side-scan sonar for underwater mapping, *Acoustic letters*, vol. 1, 1977, pp. 84-87.

[18] CLOET, R.L., S.L. HURST, C.R. EDWARDS, P.S. PHILLIPS, and A.J. DUNCAN: A sideway-looking towed depth measuring system, *Jour. of the Royal Institute of Navigation*, vol. 35, 1982, pp. 411-420.

[19] CLOET, R.L. and C.R. EDWARDS: The bathymetric swathe sounding system, *The Hydrographic Journal*, vol. 40, 1986, pp. 9-17.

[20] CLOET, R.L. and C.R. EDWARDS: The bathyscan precision swathe sounder, *Proc. MTS-IEEE Oceans'86 Conf.*, vol. 1, 1986, pp. 153-162, Washington, D.C.

[21] KLEPSVIK, J.O. and K. KLOV: Topo-SSS, a sidescan sonar for wide swath depth measurements, *Proc. Offshore Technology Conf.*, 1982, pp. 477-487.

[22] BLACKINTON, J.G., D.M. HUSSONG, and J.G. KOSALOS: First results from a combination side-scan and seafloor mapping system (SeaMARC II), *Proc. Offshore Technology Conf., OTC No. 4478*, vol. 1, 1983, pp. 307-314.

[23] HUSSONG, D.M., J.G. BLACKINTON, J.F. WILLIAMS, D. HILLS, and J.G. KOSALOS: First results of high resolution seafloor acoustic and bathymetric swath mapping system using the SeaMARC/S system, *Trans. Am. Geophys. Union, EOS*, vol. 67, no. 44, 1986, p. 1001.

[24] HARRIS, F.J.: On the use of windows for harmonic analysis with the Discrete Fourier Transform, *Proc. of the IEEE*, vol. 1, 1978, pp. 51-83.

[25] DOLPH, C.L.: A current distribution of broadside arrays which optimizes the relationship between beam width and side-lobe level, *Proc. Inst. Radio Eng.*, vol. 34, 1946, pp. 335-348.

[26] BLACKINTON, J.G.: Bathymetric mapping with SeaMARC II: an elevation-angle measuring side-scan sonar system, PhD Dissertation, University of Hawaii, Hawaii Institute of Geophysics, 1986.

[27] MACKENZIE, K.V.: Nine-term equation for sound speed in the oceans, *JASA*, vol. 70(3), 1981, pp. 807-812

[28] MAUL, G.A. and J.C. BISHOP: Mean sounding velocity, a brief review, *Int. Hydr. Rev.*, vol. 47(2), 1970, pp. 85-92.

[29] URICK, R.J.: *Principles of underwater sound, 3rd ed.*, 1983, McGraw-Hill Book Co.

[30] ALLENOU, J.P.: *Air bubbles and hull-mounted transducers (Unpublished technical report)*, 1986, GENAVIR, Brest, France.

[31] WHITE, D.J.: BO'SUN, a multibeam sonar for search and survey, *Offshore Technology Conf., OTC No. 1457*, vol. 2, 1971, pp. 393-408.

[32] RENARD, V. and J.P. ALLENOU: Sea Beam multi-beam echo-sounding in *Jean Charcot* — Description, evaluation and first results, *Int. Hydr. Rev.*, vol. 56(1), 1979, pp. 35-67, Monaco.

[33] de MOUSTIER, C. and M.C. KLEINROCK: Bathymetric artifacts in Sea Beam data: How to recognize them, what causes them, *J. Geophysical Research*, vol. 91(B3), 1986, pp. 3407-3424.

[34] POPP, D.: Improved multibeam sonar shallow water mapping system, *Proc. IEEE/MTS Oceans '84 Conf.*, vol. 1, 1984, pp. 195-199.

[35] FARR, H.K.: BO'SUN, a high resolution automatic charting system for the continental shelf, *Proc. MTS-IEEE Oceans'74*, vol. 1, 1974, pp. 10-14.

[36] PERRY, R.B.: Scientific and hydrographic use of the Bathymetric Swath Survey System, *Proc. MTS-IEEE Oceans'82 Conference*, 1982, pp. 396-401, Washington, D.C.

[37] McCAFFREY, E.K.: A review of the Bathymetric Swath Survey System, *Int. Hydr. Rev.*, vol. 58(1), 1981, pp. 19-27.

[38] de MOUSTIER, C.: Beyond bathymetry: mapping acoustic backscattering from the deep sea floor with Sea Beam, *JASA*, vol. 79(2), 1986, pp. 316-331.

[39] de MOUSTIER, C.: Approaches to acoustic backscattering measurements from the deep seafloor, in *Current practices and new technology in ocean engineering*, Ed. T. McGuinness and H.H. Shih, 1986, pp. 137-143, ASME-OED-11.

[40] OLDENBURG, G.: Honeywell Elac Bottom Chart, *Proc. IEEE/MTS Oceans'87 Conf.*, vol. 3, 1987, pp. 1190-1196.

[41] PØHNER, F.: The Simrad EM100 multibeam echosounder, a new seabed mapping tool for the hydrographer?, *13th Int. Hydrographic Conf. — Hydrographic Symposium, paper No. ES.7*, 1987, Monaco, 5-15 May 1987.

[42] HIGASHI, Y., M. OKINO, and M. TOMITA: Graphic display of seabed configuration by multibeam sonar, *Proc. MTS-IEEE Oceans '84 Conf.*, 1984, pp. 24-29, Washington, D.C.

[43] OKINO, M. and Y. HIGASHI: Measurements of seabed topography by multibeam sonar using CFFT, *IEEE Journal of Oceanic Engineering*, vol. OE-11, 1986, pp. 274-479.

[44] HAMMERSTAD, E., A. LOVIK, S. MINDE, L. KRANE, and M. STEINSET: Field performance of the Benigraph high-resolution multibeam seafloor mapping system, *Proc. MTS-IEEE Conf. Oceans '85*, vol. 2, 1985, pp. 682-685.

[45] OPPENHEIM, A.V. and R.W. SCHAFER: *Digital Signal Processing, (Ch. 6.6)*, 1975, Prentice-Hall.

[46] MATSUMOTO, H., D.M. HUSSONG, J.G. BLACKINTON, and D. HILLS: A new bathymetry processing algorithm for SeaMARC II, *Trans. Am. Geophys. Union, EOS*. vol. 66(46), 1985, p. 1072.

[47] CLOET, R.L. and C.R. EDWARDS: High resolution swathe sounding, *13th International Hydrographic Conference, Hydrographic Symposium*, Monaco, 5-15 May 1987.